Improvement in the Filtration Performance of an Ultraporous Nanofiber Membrane by Atmospheric Pressure Plasma-Induced Surface Modification

Yasuhito Mukai,* Song Liu, Yoshihiro Takayama, Yui Hayashi, Kakeru Mano, Shigenori Takahashi, Wahyudiono, Hideki Kanda, and Motonobu Goto

ACCESS | Metrics & More | Article Recommendations

ABSTRACT: Nanofiber membranes have outstanding potential for filtration applications due to their great specific surface area, high porosity, and modifiable structure. Compared to conventional membranes, nanofiber membranes offer substantial high flux and high rejection ratios. This paper provides a comprehensive analysis on the filtration performance of plasma treatment on the polyacrylonitrile nanofiber membrane. The pores in the original membrane were utilized about a mere 10%, while those of the plasma-irradiated membrane were utilized nearly 60%. The membrane modification was performed using N_2, O_2, and Ar plasma. It was found that Ar plasma was most effective for etching the membrane structure. Fourier transform infrared spectroscopy was applied to detect the chemical changes on the membranes. The contact angle of the water droplets on the original membrane was 96.1°; however, after the Ar plasma treatment, it declined to 0°. Finally, the particle retention details in different cross sections of the

filtered membranes were observed via a scanning electron microscope. The main innovation is to clarify the changes in the mechanism of the nanofiber membrane trapping particles before and after plasma treatment. In the filtration test after plasma treatment, the internal space of the membrane was fully and effectively utilized, and the flux was also improved. The obtained results suggest a potential application of the plasma-treated nanofiber membrane in water treatment.
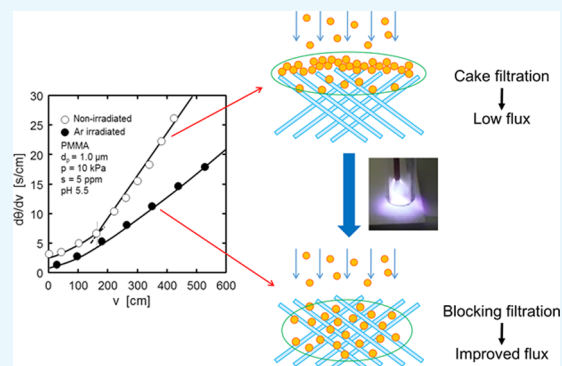
1. INTRODUCTION

Water contamination is a common problem. Considerable efforts have been devoted to developing materials, processes, and technologies, which can allow for water decontamination, management, and reuse.[1−4] Filtration, one of the most widely used methods in water treatment processes, is the operation of separating a dispersed phase of solid particles from a fluid through a porous filter medium that permits the passage of the liquid but retains the particles.[5]

The advancement of nanotechnology offers new opportunities for the development of water treatment processes. Electrospinning is a simple and reliable technique for producing continuous nanofiber (NF) membranes.[6] Small pore size, high porosity, and high surface roughness are properties that make the electrospun NF membrane a promising one in liquid filtration.[7] The electrospun NF membrane for liquid filtration has the advantages of high filtration efficiency and large flux. Heavy metals in water easily accumulate in human body and lead to serious illnesses.[8] The electrospun NF membrane can effectively remove heavy metal ions in water to improve health factors for humans.[9−11] Another feature that distinguishes it superior to the traditional

filter material is its modifiability, which can improve the selectivity, permeability, and antimicrobial properties through surface modification technologies.

Various methods, such as co-electrospinning of surface modification agents, plasma treatment, surface grafting, and wet chemical methods, were employed to modify the surface of the electrospun NF membrane.[12,13] The introduction of a transition layer to the electrospun membrane substrate is also an effective way to improve its separation and permeability properties.[14,15] Hydrophilic surface coating possesses unique advantages in treating oily wastewater.[16−18] Although both the traditional membrane and the NF membrane can obtain certain characteristics by a similar surface modification method, the NF membrane matrix has a significant advantage

in the specific surface area. Plasma treatment is regarded as a facile and environmentally benign process. Now that the mass production technology of NF membranes has become increasingly mature, it is envisioned that the integration of a plasma irradiation device into the industrial membrane manufacturing device will make the production of batch plasma-treated membranes economically practical. Plasma is described as the fourth state of matter composed of electrons, radicals, photons, and ions positively or negatively charged. Suitable gas sources such as H_2, O_2, and N_2 can be used to functionalize the NF surface.[19] As an efficient technique to introduce a selective polymeric layer on the surface of a hydrophobic membrane, plasma-induced graft copolymerization treatment is limited to the surface, and the thickness of the modified layer can be controlled down to an angstrom level.[20] Thus, the surface property can be customized to meet a specific requirement, while maintaining the bulk properties of membranes. Mozaffari et al. functionalized gelatin NFs with argon and argon−oxygen plasmas.[21] After argon−oxygen plasma treatment, the surface of the resultant NF became completely hydrophilic. Yalcinkaya observed the permeability of the neat and plasma-treated polyvinylidene fluoride (PVDF) NF membranes for the separation of wastewater. The PVDF membranes became hydrophilic/oleophobic after the plasma treatment and exhibited a higher permeability than the neat samples. However, the duration of the plasma effect for the permeation test was unsatisfactory.[22] Padil et al. evaluated the adsorption capacities of the deacetylated gum kondagogu and polyvinyl alcohol NFs for the extraction of nanoparticulate silver, gold, and platinum.[23] They indicated that the higher surface area of the plasma-treated NFs leads to a higher extraction efficiency than that of the untreated NFs. Relative to chemical treatment methods, such as alkali treatment to increase the wettability of the membrane,[24] the plasma treatment is much greener because it does not use chemical reagents. Polyacrylonitrile (PAN) is an ideal polymer for electrospinning with the features of easy transformation to a fiber-type shape, high flexibility in structure control, and good stability in different environments.[25] The modified PAN NF has been extensively studied for the adsorption of toxic metals, water filtration, skincare, and other applications.[26] However, the hydrophilicity of the PAN NF membrane is insufficient for use as a filter medium.

Membrane filtration can be classified into surface filtration and depth filtration according to the particle trapping mechanism. Also, surface filtration is also named cake filtration because deposited particles form filter cake layers on the membrane surface. Cake structure analysis has been widely studied in the cake filtration. For example, the authors' research group has conducted detailed studies on the effects of sample solution conditions such as pH,[27,28] ionic strength,[28] solvent type,[29] and particle concentration[30] on the formation of a cake structure. On the other hand, in depth filtration, particles penetrate into the membrane pores and block the pores, which is called blocking filtration. The research on blocking filtration mainly focuses on the development of blocking filtration models in the blocking filtration process. Up to now, various blocking filtration models[31−33] and combined models of blocking filtration and cake filtration[34−36] have been proposed.

This study aims to apply plasma to modify the PAN NF membrane for use as a filter medium. The influence of plasma effects on filtration behavior and solid particle occupancy ratio

inside the NF layer has been investigated. The plasma effects of different gas sources are presented. The stability of the membrane after plasma treatment was also examined. The chemical structure of the plasma-irradiated PAN NF membranes was detected by Fourier transform infrared spectroscopy measurement. The changes of the membrane surface wettability were examined by contact angle measurement. In the end, the particle retention details in different cross-sections of the filtered membranes were observed via a scanning electron microscope. The main innovation is to clarify the changes in the mechanism of NF membrane trapping particles before and after plasma treatment.

2. RESULTS AND DISCUSSION

2.1. Effects of Particle Diameter on Filtration Performance. Filtration operations are divided into two main categories: cake filtration and depth filtration. In cake filtration, particles in a slurry form a deposit as a filter cake on the surface of the supporting porous medium, while the fluid passes through it.[33] After an initial period of deposition, the filter cake itself starts to act as the filter medium, while further particles are deposited. The structure of the formed cake and its resistance to liquid flow depend on the properties of the solid particles, the liquid-phase suspension, and the filtration conditions. According to Ruth,[37] when filtration conforms to the cake filtration mechanism, the relationship between the cumulative filtrate volume collected per unit effective area v (cm^3/cm^2) and the filtration time θ can be described by the following equation, where the time variation curve of filtrate volume is a parabola.

$$(v + v_m)^2 = K_v(\theta + \theta_m) \tag{1}$$

where v is the cumulative filtrate volume collected per unit effective area (cm^3/cm^2), v_m is the fictitious filtrate volume per unit membrane area (cm^3/cm^2), equivalent to the flow resistance of the membrane, K_v is the Ruth filtration coefficient (cm^2/s), θ is the filtration time (s), and θ_m is the fictitious filtration time (s), equivalent to the flow resistance of the membrane. Differentiating eq 1, the following equation is obtained after finishing.

$$\frac{d\theta}{dv} = \frac{2}{K_v}(v + v_m) \tag{2}$$

where $(d\theta/dv)$ is the reciprocal filtration rate. In other words, the graph is linear when plotting the reciprocal filtration rate versus the filtrate volume according to eq 2. This graphing method is called the Ruth plot and is often used to analyze the cake filtration.

Depth filtration is also known as filter medium filtration or clarifying filtration. In depth filtration, particles are captured within the complex pore structures of the filter medium, and the cake is not formed on the surface of the medium. In many processes, a stage of depth filtration precedes the formation of a cake. The first particles can enter the medium, and with very dilute slurries, there can be a time lag before a cake begins to form. Smaller particles enter the medium, whereas larger particles bridge the openings and start the buildup of a surface layer. Hermans and Bredée[38] assumed that the filter medium is an aggregate of capillaries with consistent length and diameter and modeled the pore blocking process for depth filtration. Assuming that particles smaller than the capillary diameter are uniformly adhered to the inner wall of the capillary and the
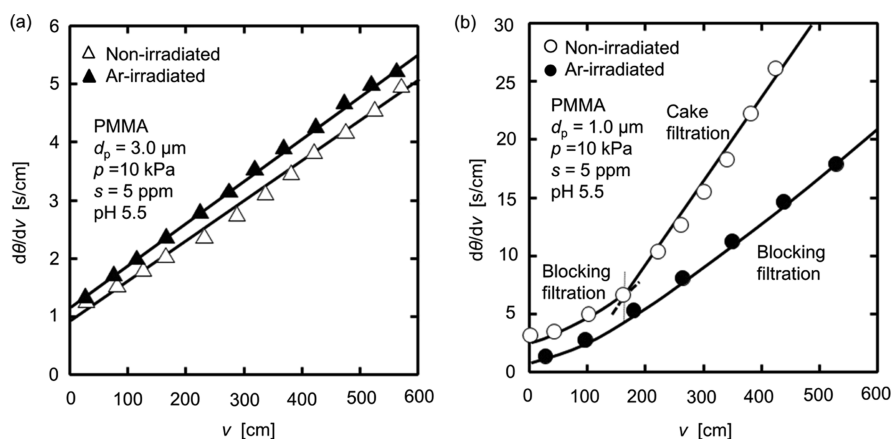
Figure 1. Filtration behaviors of the original and the Ar-irradiated PAN NF membranes for (a) 3 μm PMMA particles and (b) 1 μm PMMA particles.
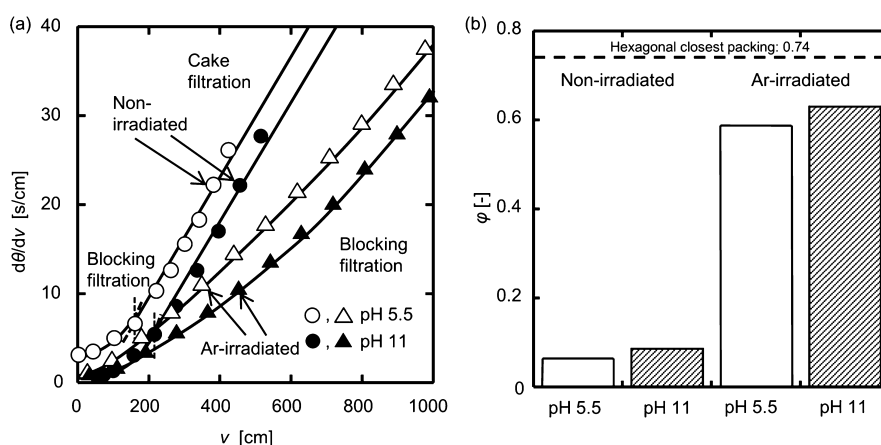
Figure 2. pH effect on (a) filtration behaviors and (b) internal occupancy ratio φ for the original and the Ar-irradiated PAN NF membranes.

inner diameter of the capillary gradually decreases, the relationship between the filtration rate $(\mathrm{d}v/\mathrm{d}\theta)$ and the filtrate volume v is derived from the following equation

$$\frac{\mathrm{d}v}{\mathrm{d}\theta} = \left(\frac{\mathrm{d}v}{\mathrm{d}\theta}\right)_0\left(1 - \frac{K_s}{2}v\right)^2 \tag{3}$$

where K_s is the blocking filtration coefficient (1/cm). This type of pore blocking pattern is referred to as the standard blocking law. In addition, when eq 3 is graphed using the Ruth plot $(\mathrm{d}\theta/\mathrm{d}v \text{ vs } v)$, it becomes a curve that is convex downward.

Figure 1 presents filtration behaviors of the original and the Ar-irradiated PAN NF membranes for 3 μm polymethyl methacrylate (PMMA) particles and 1 μm PMMA particles. The rejection ratios of the NF membranes to both types of the PMMA particles were 100%. The slope of the reciprocal filtration rate versus filtrate volume shown in Figure 1a remains constant, which is consistent with the mathematical description for filtration in eq 2, showing a typical cake filtration process. It is revealed that 3.0 μm particles were wholly trapped on the upper surface in the filtration process of the two membranes. This is because the particle diameter was larger than the pore diameter of the membranes, and thus, the particles could not get into the inner pores of the membranes. Plasma irradiation did not affect this case, indicating that the particles in the experiment were too large. Therefore, it is necessary to choose smaller particles to study the impact of plasma treatment. Figure 1b displays reciprocal filtration rate versus filtrate

volume in the filtration of 1.0 μm PMMA particles. At the initial stage of filtration, the reciprocal filtration rate of the original membrane increased slowly with the filtrate volume, indicating that the pores of the membrane were being blocked. However, after a short period, the reciprocal filtration rate increased linearly with respect to the filtrate volume. According to eq 2, the filtration process entered the cake filtration stage. The sharp decrease of flux during this stage was attributed to the great increase in cake resistance. On the other hand, the process of filter cake formation was much longer in the Ar plasma-irradiated membrane. In the experimental filtrate volume range, the reciprocal filtration rate of the Ar plasma-irradiated membrane rose slowly according to the filtrate volume. It is evident from the changing slope that the pores of the Ar plasma-irradiated membrane were gradually blocked but not completely closed. Though the ultraporous structure was partially blocked, the flux did not drop rapidly because the flow of other channels was sufficiently secured. The Ar plasma treatment improved the morphology of the PAN fiber surface, causing the particles to infiltrate into the membrane pores and delaying the formation of the filtration cake. In the following filtration experiments, 1.0 μm PMMA particles were used to examine the plasma modification effect for the membranes.

2.2. Effect of pH on Filtration Performance. The cake structure is determined by hydrodynamic factors, cake porosity, mean particle size, size distribution, particle specific surface area, and sphericity. Moreover, it is also strongly

influenced by some physico-chemical factors.[39] The influence of physico-chemical factors is closely related to surface phenomena at the solid−liquid boundary. For fine particle suspensions, colloidal forces control the nature of the filter cake. The repulsive electrostatic forces will vary with the surface charge of the suspended particles, which varies with the solution environment. Therefore, the filtration behaviors of the colloids are affected significantly by the solution properties, including pH and electrolyte strength. Surface electrical potential is a function of the change in pH.[40] Solution pH affects the structure and surface charge of the solute, as well as the membrane surface properties, thus affecting the interaction between the solute and the membrane surface, the deposition amount of the solute on the membrane, and the flux of the membrane. Figure 2 displays the pH effect on filtration behaviors and internal occupancy ratio φ for the original and the Ar-irradiated PAN NF membranes. The internal occupancy ratio φ reveals the intrusion of solid particles in the internal space of the filter media and also provides evidence for the filtration performance improvement and the occurrence of blocking filtration. The zeta potentials of PMMA particles at pH 5 and pH 11 were measured to be −37 and −58 mV, respectively; those of the PAN NF membrane were measured to be −24 and −30 mV, respectively. Thus, the zeta potentials of PMMA particles and the membrane surface become more negative from pH 5 to pH 11, and the electrostatic repulsion between the PMMA particles and the membrane surface is greater at pH 11 than at pH 5.

As shown in Figure 2a, the blocking period in the pH 11 suspensions was slightly longer than that in the pH 5 suspensions for the original membranes, whereas blocking filtration of the Ar-irradiated membranes persisted for the duration of the filtration process at pH 5 and pH 11. Figure 2b displays the internal occupancy ratio φ for the filtered membranes calculated from eq 9 (described in Section 4.6). The PMMA particles used were spherical and uniform in size, so if the entire space inside the pore was occupied by PMMA particles in a dense state, the occupancy ratio would be 0.74 from the perspective of the hexagonal closest packing.[41,42] Therefore, 0.74 was taken as the maximum value, and the effect of filtration performance improvement was evaluated according to how close the occupancy ratio could get to it. The pores in the original membrane were utilized about a mere 10%, while those of the plasma-irradiated membrane were utilized nearly 60%, and most of the internal pores of the membrane were occupied by PMMA particles. The utilization of the internal space was significantly improved by plasma treatment. The flux of the original membrane was a little larger at pH 11 than at pH 5, attributed to a slight prolongation of the blocking filtration period. In contrast, the plasma-treated membranes exhibited a significant increase in the flux and had a longer blocking filtration period. It is obvious that plasma treatment has an overwhelming superiority over the pH value in terms of flux increase.

2.3. Comparison of Filtration Performance for the MF Membrane and the PAN NF Membrane. Microfiltration (MF) membranes and NF membranes cover almost the same particle size range for suspension filtration.[43,44] Therefore, the filtration performance of both membranes irradiated by Ar plasma was compared. The permeability of PMMA particles was zero for both MF and NF membranes. Figure 3 displays the filtration behaviors of the MF membranes and the PAN NF membranes with and without plasma irradiation. The Ar-
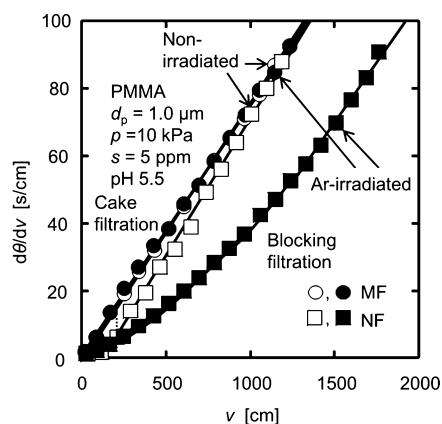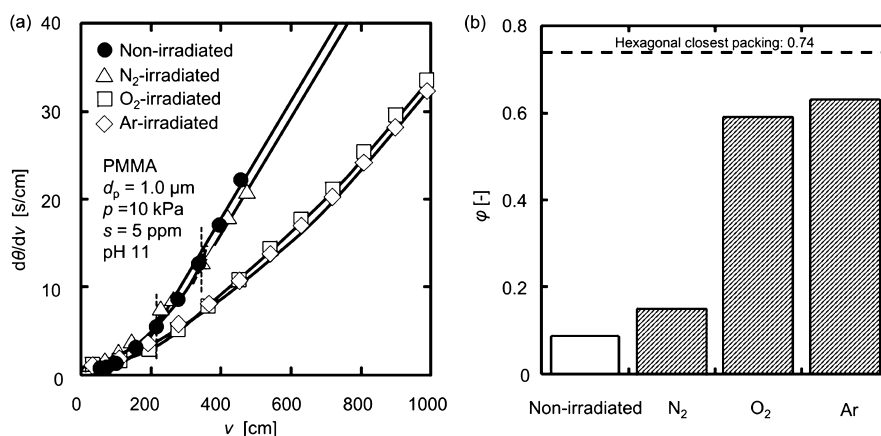

Figure 3. Filtration behaviors of the MF membranes and the PAN NF membranes with and without plasma irradiation.

irradiated PAN NF membrane exhibited a blocking filtration in the experimental range, while the MF membranes showed a cake filtration, and the original PAN NF membrane transformed into cake filtration after a short period of blocking filtration. That is because the porosity of the MF membranes was lower than that of the NF membrane; particles could not enter the filter interior and were trapped near the inlet of the pores. Thus, the plasma irradiation was ineffective for the MF membrane in the test. The treatment of the PAN NF membrane by Ar plasma delayed the formation progress of the filter cake and promoted flux improvement distinctly.

2.4. Effect of Plasma Resource on Filtration Performance of the PAN NF Membrane. The PAN NF membranes were irradiated using plasma generated by N_2, O_2, and Ar. The resulting membranes were used to filter the 1.0 μm PMMA suspensions to assess the effects of the plasma resource. Figure 4a displays the effect of the plasma gas type on filtration behaviors for the original and the irradiated PAN NF membranes. The N_2 plasma-irradiated NF membrane showed a slight improvement in filtration performance compared to the original membrane; nevertheless, the effect was not as significant as that of the O_2 and Ar plasma-irradiated membranes. Figure 4b displays the internal occupancy ratio φ of the four membranes after filtration. According to the order of occupancy ratio φ, the modification effect of the NF membrane varies with the plasma gas type, and the ranking of the modification effect is Ar, O_2, and N_2. The Ar plasma was more energetic and the O_2 plasma carried its own oxygen-containing groups,[45−47] so that better treatment effects were obtained than that of the N_2 plasma treatment process.

2.5. Plasma Penetration Depth. The internal occupancy ratio study of the filtered membranes in Sections 2.2 and 2.4 shows that the plasma modification is effective not only on the irradiated surface but also on the interior. To ensure a uniform plasma treatment effect on the surfaces of fibers, the reactive species must penetrate the inner structure in an acceptable duration of treatment time. Good penetration of plasma effects into the internal structure is crucial for successful plasma modification.[48] Therefore, the penetration depth of the Ar plasma to the interior of the PAN NF membrane was studied in this research.

The thickness of a single membrane was 0.12 mm; four NF membranes were laminated together and then irradiated with Ar plasma from the top face. The 1.0 μm PMMA suspension was filtered separately by the irradiated membrane from each

Figure 4. Effect of the plasma gas type on (a) filtration behaviors and (b) internal occupancy ratio φ for the original and the irradiated PAN NF membranes.
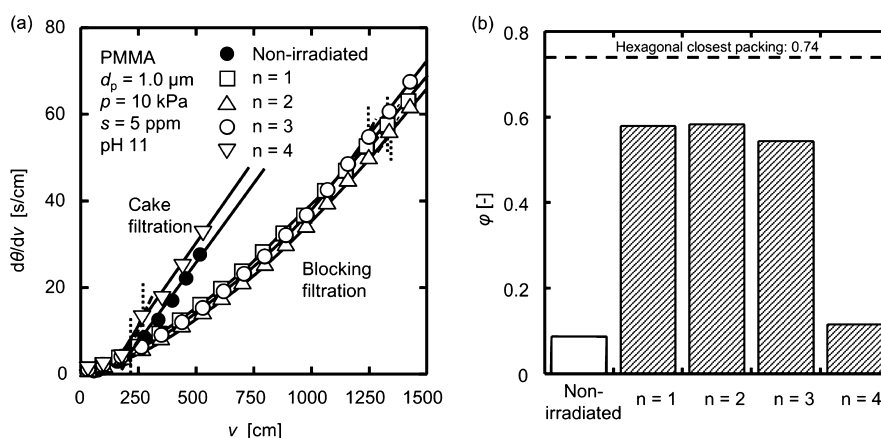

Figure 5. Comparison of (a) filtration behaviors and (b) internal occupancy ratio φ for the original membrane and the irradiated PAN NF membranes from different layers during the batch plasma treatment.

layer. The reciprocal filtration rate versus filtrate volume is shown in Figure 5. Among the four NF films stacked, the one closest to the plasma irradiation is noted as $n = 1$ and then increased sequentially, with the fourth being the farthest. The formation of the cake layer was delayed by plasma irradiation in the first three membranes. Nevertheless, the filtration behavior of the fourth was very close to that of the original membrane because the filtration performance was not improved. Figure 5b displays the internal occupancy ratio φ of the irradiated membranes from different layers. The first two irradiated membranes had the highest internal occupancy ratio, while the third decreased slightly. The fourth had the lowest internal occupancy ratio, which was almost in line with that of the original membrane. The reactive species created in the plasma were transported toward the substrate, and naturally, the probability of the top membrane was higher than that of the lower membranes.[49] As the layer number increased, the treatment dose decreased due to the reduced number of active species that could penetrate through the layers.[50] Therefore, it is confirmed that plasma irradiation can penetrate the depth of three membranes and etch the membrane's internal structure. Additionally, the irradiation depth study serves as an inspiration for the batch plasma treatment of the membrane.

2.6. Sustainability of Modification Effects by the Plasma Treatment. Plasma treatment is a low cost and clean technology to improve the physical and chemical properties of

NF membranes. The aging of the modified surface is a challenge in the plasma treatment of polymers. The instability of plasma-treated materials after a certain time has also been reported.[22,51,52] The polymer surface is driven away from its thermodynamic equilibrium by developing concentration gradients of polar groups in the surface region or the sub-surface region in the plasma treatment. After treatment, the modified surface reconstructs in order to minimize its surface energy and to return to an equilibrium state with storage time.[53] The kinetics of these surface dynamics are influenced by many factors, including plasma parameters, molecular structure, and storage conditions. The PAN NF membranes irradiated with Ar plasma were stored in a dark and dry place away from sunlight and excessive humidity. Then, they were used to filter suspensions containing 1.0 μm PMMA particles, and the filtration results are shown in Figure 6. With the elongation of the storage time, the filtration performance of the membranes stored for 15 and 25 days showed different degrees of degradation compared to the membrane stored for only 1 day. In spite of this, with the storage of 25 days, the filtration performance of the membranes was substantially better than the original membrane. Therefore, Ar plasma can improve the filtration performance of the NF membrane for a satisfactory amount of time. The preservation of the filtration performance is mainly due to the etching effect of Ar plasma on the NFs. Still, the weak degradation with storage time is related to the
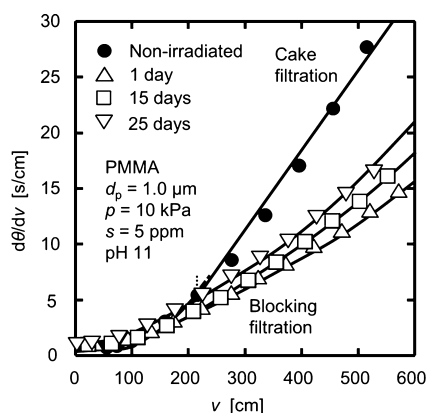
Figure 6. Filtration behaviors of the original membrane and the irradiated PAN NF membranes with different storage times.

hydrophobic recovery caused by the decrease of the surface energy.

Wavhal and Fisher[54] and Yalcinkaya[22] observed the changes in the contact angle of membranes after plasma treatment within 2 and 55 days, respectively. The contact angle increased over time; however, the hydrophilicity gained during surface treatment did not disappear completely. It is worth noting that it is impossible to completely avoid the aging process. The sustainability study can help confirm the search for the modified membrane's storage validity and optimize the plasma treatment process. The assessment of the ambient storage lifetime is of interest for future research. In addition, prolonging of the treatment effect is one of the next research directions, such as dipping the plasma-treated membranes in polymer solutions bearing free radical couplable functional groups.
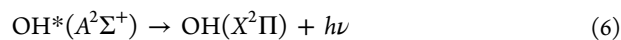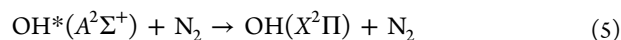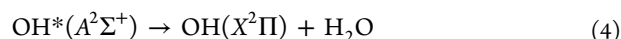
2.7. Observation of Plasma by Optical Emission Spectroscopy. Optical emission spectroscopy was used to record the spectra of the Ar plasma. Figure 7 shows the spectra
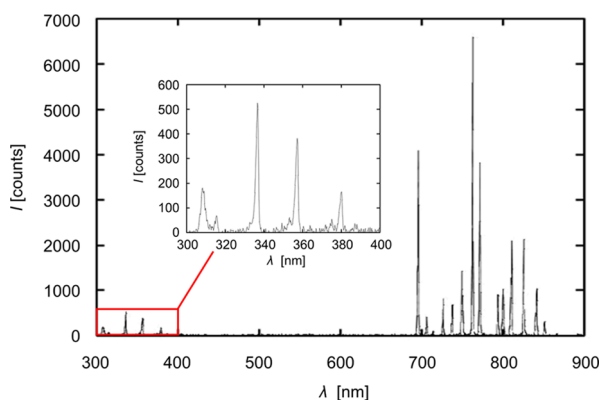

Figure 7. Optical emission spectra of the Ar plasma.

results of the Ar plasma inside the glass tube over a wavelength of 300−900 nm. The spectra are mainly composed of neutral argon lines in the red/near-infrared spectral region 690−900 nm that belongs to transitions from the $3p^54p$ to $3p^54s$ configuration.[55] The Ar plasma can etch the membranes and modify the fiber structure and pores. The N_2 emission line $[C^3\Pi u \rightarrow B^3\Pi g(0,0)$ at 337 nm] suggests that N_2 in the atmosphere near the plasma nozzle was generated by Ar plasma.[56] The optical emission spectroscopy of OH radicals

during the discharge mainly appears near 309 and 314 nm by the processes as follows[57]

$$OH*(A^2\Sigma^+) \rightarrow OH(X^2\Pi) + H_2O \tag{4}$$

$$OH*(A^2\Sigma^+) + N_2 \rightarrow OH(X^2\Pi) + N_2 \tag{5}$$

$$OH*(A^2\Sigma^+) \rightarrow OH(X^2\Pi) + h\nu \tag{6}$$

As shown in the enlargement in the wavelength range 300−400 nm, the optical signals of OH radicals were collected by optical emission spectroscopy. It is considered that OH radicals were derived from the excited moisture. From the enhanced filtration behavior after the plasma treatment, it can be speculated that the reactive characteristic of OH radicals was also one of the factors at play.[47,58]

2.8. FTIR Analysis. The possible changes in the PAN NF membrane's chemical structure after the plasma irradiation were detected by the FTIR spectra. Figure 8 displays the FTIR
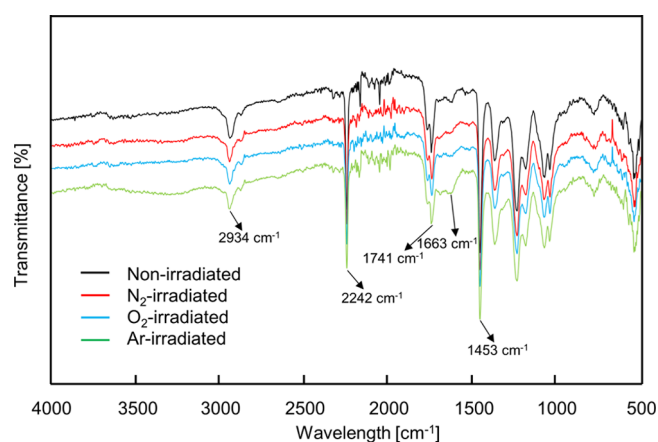
Figure 8. FTIR analysis of the original membrane and the $N_2/O_2/Ar$-irradiated PAN NF membranes.

spectra of the original membrane and the $N_2/O_2/Ar$ plasma-irradiated membranes. The prominent peaks for PAN around 2934, 2242, 1741, and 1663 cm^{-1} correspond to the stretching vibrations of the −CH, −C≡N, −C═O, and −C═N groups, respectively.[59,60] Moreover, the strong peak at 1453 cm^{-1} is assigned to the bending vibration of the −CH$_2$ group. During the plasma irradiation, C≡N bonds of the original PAN NF membranes were not broken. No significant changes were observed between the original and the plasma-treated membranes. Although the plasma treatment effect was both structural and chemical, FTIR was difficult to detect the difference because the population of surface functional groups is insignificant compared to the bulk functional groups of original PAN. The membranes treated by plasma only involved superficial changes, on the order of nanometers.[22] The superficial changes were not photographed because the SEM S4300 has difficulty in capturing objects with sizes less than 10 nm.

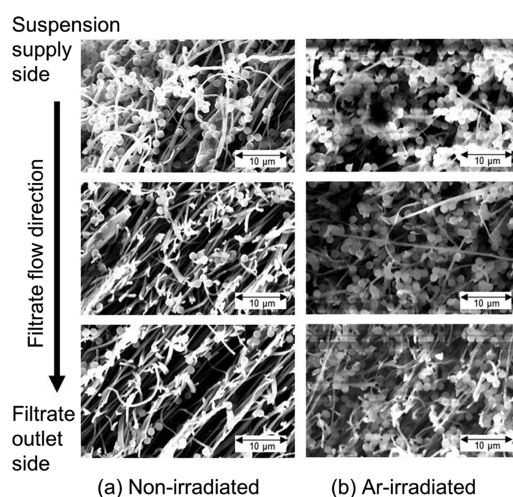**2.9. Hydrophilicity Evaluation of the Modified NF Membrane.** Contact angle measurements were performed on the original and the plasma-treated PAN NF membranes to determine the effect of plasma treatment on the hydrophilicity of the membrane surface. Measurement of the contact angle was performed 2.5 s after a 1.0 μL drop of deionized water was injected onto the membrane surface. Figure 9 presents the
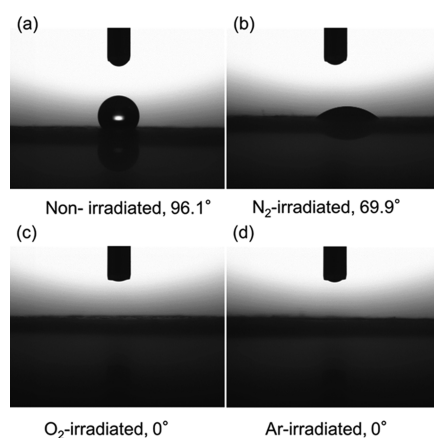
Figure 9. Contact angles of water droplets on (a) original membrane, (b) N_2-irradiated PAN NF membrane, (c) O_2-irradiated PAN NF membrane, and (d) Ar-irradiated PAN NF membrane.

Figure 10. SEM photographs of the different cross-sections of (a) filtered original membrane and (b) filtered Ar-irradiated PAN NF membrane.

difference between the contact angles of the PAN NF membranes before and after the plasma irradiation. The contact angle of the water droplets on the original membrane was 96.1°. After N_2 plasma treatment, the contact angle value reduced to 69.9°. Water droplets thoroughly infiltrated the surface of the membranes irradiated by O_2 and Ar plasma, and no contact angle could be obtained. Wang et al. reported the contact angle of the polyphenylsulfone NF membranes changed from 137 to 0°.[61] The contact angle measurements were also unable to be performed in their research because the water drop disappeared into the membrane immediately. It can be considered that a surface with a contact angle between 0 and 30° is hydrophilic, while a hydrophobic surface is characterized by a contact angle greater than 90°.[62] The enhancement of the material wettability mainly comes from the changes in the surface chemical structure and in surface roughness.[63,64] The chemical structure changes specifically refer to the plasma-induced formation and subsequent incorporation of polar groups on the NF surface. Additionally, the polar OH radical was detected in the optical emission spectroscopy study of 3.7. The results indicated that the surface wettability of the PAN NF membranes has dramatically increased from the plasma treatment.

2.10. SEM Analysis. In order to observe the capture of particles inside the membrane in detail, the cross-sections of the original and the Ar plasma-irradiated membranes were photographed by SEM along with the upstream, middle, and downstream of the filtrate flow direction at $v = 1300$ cm. Figure 10 presents the existence of PMMA particles inside the membranes. As shown in Figure 10a, PMMA particles were captured in the surface and upper of the membrane; almost no particles are observed in the middle and lower layers in the original membrane, indicating that the cake layer formed prematurely in the upper surface of the original membrane, which corresponds to the result that the internal occupancy ratio φ was only 10% in Section 2.2. On the other hand, as shown in Figure 10b, PMMA particles existing in the pores of the NFs were not only in the upper layer but also in the middle and lower layers, supporting the result regarding the internal occupancy ratio φ of about 60% in the previous section. Because no PMMA particles penetrated into the filtrate, the PMMA rejection ratios were 100%, demonstrating that no large changes in the pore size of the plasma-treated membrane occurred. The changes in the particle capture mechanism were

not caused by changes in the pore size of the membrane. It is further confirmed that plasma plays a role in reshaping the membrane's internal structure and delaying the cake layer formation in the filtration process. The inner capturability of solid particles also shows a prospect of the plasma-treated NF membrane for the depth filtration process.

3. CONCLUSIONS

NF membranes with the characteristics of high surface area and high porosity offer better liquid filtration at lower energy costs than conventional filtration materials. In this research, plasma from different gas sources was applied to modify PAN NF membranes. The filtration experiments of PMMA particle suspension were conducted to verify the performance change of the membrane before and after the plasma treatment. The Ar plasma treatment changed the morphology of the PAN NF surface, led the particles to infiltrate into the membrane pores, and delayed the formation of the filtration cake. After comparing the filtration behavior of the membranes irradiated with plasma from different gas sources and analyzing the internal solid particle occupancy ratio of the filtered membranes, it was found that Ar plasma treatment obtained a more beneficial improvement effect than that of N_2 or O_2. The batch plasma irradiation treatment of several membranes stacked on top of each other shows that the improvement of the fiber structure by plasma not only is limited to the membrane surface but also penetrates to the membrane interior. The maximum penetration depth for the batch Ar plasma irradiation was up to three membranes at a time, which was 0.36 mm. The contact angle of the membranes decreased significantly after the plasma treatment, and the enhancement of surface wettability is highly desirable. In addition, the SEM images displayed the retention details of the PMMA particles inside the filtered membranes. The present work demonstrated that the surface modification of the NF membrane by plasma treatment enormously improved the flux advancement during the filtration process. The upgrading of the internal particle trapping effect by the plasma treatment makes the NF membrane a bright prospect in the water treatment field.

4. MATERIALS AND METHODS

4.1. Materials. The electrospun PAN NF membrane was supplied by Japan Vilene Company, Ltd., Japan. The average fiber diameter of the NF membrane is about 411 nm, and the fiber mass per unit area is 17.3 g/m^2. The thickness of the NF membrane is 0.12 mm. The average hydraulic equivalent diameter of the NF membrane was obtained as 2.3 μm by measuring the time-dependent variation of the permeate volume per unit permeate area through the water permeation tests at different pressures, which was according to JIS R 1671 (Japanese Industrial Standards, testing method for water permeability and hydraulic equivalent diameter of porous fine ceramics). Also, the measured pore size of the Ar-irradiated NF membrane was 2.3 μm, unchanged compared to the NF membrane before plasma treatment. The MF cellulose ester membrane with a nominal size of 3.0 μm was supplied by Advantec Co., Ltd., Japan. The manufacturers guarantee a sharp pore size distribution for the membranes. Two types of monodispersed PMMA microspheres with nominal diameters (d_p) of 1.0 and 3.0 μm were purchased from Sekisui Kasei Co., Ltd., Japan. 1 M NaOH solution was purchased from Wako Pure Chemical Industries, Ltd., Japan.

4.2. Filtration Experimental Equipment. Figure 11 outlines the schematic diagram of the filtration experimental
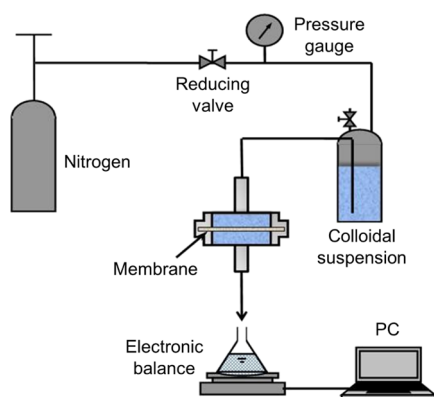
Figure 11. Schematic diagram of the filtration experimental apparatus.

apparatus. The filtration system consists of a nitrogen cylinder, stainless-steel pressurized vessel, filter holder, electronic balance, and other parts. The PAN NF membrane with a diameter of 2.5 cm was packed in the Advantec filter holder (LS-25) with an effective diameter of 2.2 cm and a permeation area of 3.8 cm^2. The nitrogen pressure was adjusted by a valve, and then, the pressure (p = 10 kPa) was applied to the colloidal suspension tank and the filter. Filtration experiments were performed by measuring the change in filtrate volume versus time using the electronic balance. The filtrate volume data were collected by the PC connected to the electronic balance.

4.3. Plasma Equipment. The PAN NF membranes were irradiated by the plasma of the various gases of N$_2$/O$_2$/Ar for 6 min at atmospheric pressure. The schematic of the plasma treatment configuration is shown in Figure 12. The plasma system consists of a bipolar impulse waveform generator (HVP1010K300-NP, Tamaoki Electronics Co., Ltd., Kawaguchi, Japan), high voltage probe (EP-50K, Nissin Pulse Electronics Co., Ltd., Chiba, Japan), digital oscilloscope (TDS-2024C, bandwidth 200 MHz, Tektronix Inc., OR, USA), gas
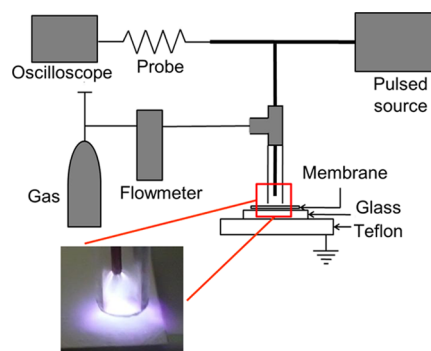
Figure 12. Atmospheric pressure plasma irradiation equipment.

cylinder, and Teflon plate. The length of the electrode was 75 mm, and the quartz glass tube surrounding the electrode had an inner diameter of 3.5 mm, an outer diameter of 5.0 mm, and a length of 80 mm. The electrodes are made of copper with a diameter of 1 mm and sides covered with polyether ether ketone. The distance between the edge of the quartz glass tube and the PAN NF membrane was 10 mm. Therefore, the luminescent jet length was about 15 mm. The electrode was powered by the bipolar impulse waveform generator with a repetition frequency of 10 kHz with the applied voltage amplitude of 10.0 kV. The gas flow rate was fixed at 150.0 mL/min, controlled by the flow controller. The membrane samples were placed on the glass slide. Then, the samples were irradiated by plasma with a moving speed of 1 mm/s in a quartz glass tube.

4.4. Preparation of PMMA Suspension. PMMA particles were added to deionized water to prepare a suspension with the mass fraction of 5 ppm. NaOH solution was added to adjust the pH value for the suspension of pH = 11. Then, the suspension was stirred with a magnetic stirrer at 300 rpm for 30 min. Next, the suspension beaker was placed in an ultrasonic cleaner and irradiated with ultrasonic waves at 28 kHz for 10 min, followed by stirring with a magnetic stirrer for 10 min. The ultrasonic irradiation and stirring operations were repeated two to three times to make the PMMA particles well dispersed and homogeneous. The PMMA concentrations of the sample suspension and the permeate were measured by an ultraviolet spectrophotometer (UV-1800, Shimadzu). The detection wavelength is 240 nm for PMMA with a diameter of 3.0 μm and 460 nm for PMMA with a diameter of 1.0 μm.

4.5. Characterization. Spectroscopic analysis of optical emission during the plasma treatment was performed by an optical emission spectrometer (HR4000, Ocean Optics, Japan). Then, the surface chemical functional groups of the PAN NF membranes were investigated by Fourier transform infrared spectroscopy (FTIR, Spectrum Two, PerkinElmer, Japan) in the region of 4000−500 cm^{-1}. The water contact angle of the membrane samples was assessed by a contact angle meter (DM 501, Kyowa Interface Science, Japan) equipped with an image capturing system. Scanning electron microscopy (SEM, S4300, Hitachi, Japan) was used to observe the surface morphology of the PAN NF membranes.

4.6. Internal Occupancy Ratio of the Membrane. The apparent density ρ_b of the PAN NF membrane is defined as

$$\rho_b = \frac{w}{L} \tag{7}$$

where w (=17.3 g/m^2) is the fiber mass per unit area of the NF membrane and L (=0.12 mm) is the thickness of the NF membrane. The porosity of the membrane is given by

$$\varepsilon = 1 - \frac{\rho_b}{\rho_{PAN}} \tag{8}$$

where ρ_{PAN} (=1.17 g/cm^3) is the density of the PAN. ε was calculated as 0.88 by substituting eq 7 into eq 8.

In order to study the utilization extent of the internal pore, the internal occupancy ratio φ, defined as the ratio of the volume of all captured particles inside the filter medium to the pore volume inside the filter medium, is given by the following equation:

$$\varphi = \frac{\rho_s(L\varepsilon + v_b)}{[\rho_p(1 - s) + \rho_s]L\varepsilon} \tag{9}$$

where ρ_p (=1.2 g/cm^3) and ρ (g/cm^3) are the densities of the PMMA particle and filtrate liquid, respectively. s is the mass fraction of solids in the suspension, and v_b is the filtrate volume during the blocking filtration, from the beginning of the blocking filtration until the shift to cake filtration.

AUTHOR INFORMATION

Corresponding Author

Yasuhito Mukai − *Department of Chemical Systems Engineering, Nagoya University, Nagoya 4648603, Japan;* orcid.org/0000-0001-6338-2315;
Email: mukai.yasuhito@material.nagoya-u.ac.jp

Authors

Song Liu − *Department of Chemical Systems Engineering, Nagoya University, Nagoya 4648603, Japan*

Yoshihiro Takayama − *Department of Chemical Systems Engineering, Nagoya University, Nagoya 4648603, Japan*

Yui Hayashi − *Department of Materials Process Engineering, Nagoya University, Nagoya 4648603, Japan*

Kakeru Mano − *Department of Materials Process Engineering, Nagoya University, Nagoya 4648603, Japan*

Shigenori Takahashi − *Department of Materials Process Engineering, Nagoya University, Nagoya 4648603, Japan*

Wahyudiono − *Department of Materials Process Engineering, Nagoya University, Nagoya 4648603, Japan;* orcid.org/0000-0003-0339-1740

Hideki Kanda − *Department of Materials Process Engineering, Nagoya University, Nagoya 4648603, Japan;* orcid.org/0000-0002-8393-4276

Motonobu Goto − *Department of Materials Process Engineering, Nagoya University, Nagoya 4648603, Japan;* orcid.org/0000-0003-3219-5028

Complete contact information is available at:
https://pubs.acs.org/10.1021/acsomega.1c04044

Author Contributions

The manuscript was written through contributions of all authors. All authors have given approval to the final version of the manuscript.

Notes

The authors declare no competing financial interest.

REFERENCES

(1) Tang, C. Y.; Yang, Z.; Guo, H.; Wen, J. J.; Nghiem, L. D.; Cornelissen, E. Potable water reuse through advanced membrane technology. *Environ. Sci. Technol.* **2018**, *52*, 10215−10223.

(2) Kumar, M.; Singh Dosanjh, H.; Sonika; Singh, J.; Monir, K.; Singh, H. Review on magnetic nanoferrites and their composites as alternatives in waste water treatment: synthesis, modifications and applications. *Environ. Sci.: Water Res. Technol.* **2020**, *6*, 491−514.

(3) Chenab, K. K.; Sohrabi, B.; Jafari, A.; Ramakrishna, S. Water treatment: functional nanomaterials and applications from adsorption to photodegradation. *Mater. Today Chem.* **2020**, *16*, 100262.

(4) Marsidi, N.; Abu Hasan, H.; Sheikh Abdullah, S. R. A review of biological aerated filters for iron and manganese ions removal in water treatment. *J. Water Process Eng.* **2018**, *23*, 1−12.

(5) Hube, S.; Eskafi, M.; Hrafnkelsdóttir, K. F.; Bjarnadóttir, B.; Bjarnadóttir, M. Á.; Axelsdóttir, S.; Wu, B. Direct membrane filtration for wastewater treatment and resource recovery: a review. *Sci. Total Environ.* **2020**, *710*, 136375.

(6) Ahmed, F. E.; Lalia, B. S.; Hashaikeh, R. A review on electrospinning for membrane fabrication: challenges and applications. *Desalination* **2015**, *356*, 15−30.

(7) Cui, J.; Li, F.; Wang, Y.; Zhang, Q.; Ma, W.; Huang, C. Electrospun nanofiber membranes for wastewater treatment applications. *Sep. Purif. Technol.* **2020**, *250*, 117116.

(8) Efome, J. E.; Rana, D.; Matsuura, T.; Lan, C. Q. Insight studies on metal-organic framework nanofibrous membrane adsorption and activation for heavy metal ions removal from aqueous solution. *ACS Appl. Mater. Interfaces* **2018**, *10*, 18619−18629.

(9) Efome, J. E.; Rana, D.; Matsuura, T.; Lan, C. Q. Experiment and modeling for flux and permeate concentration of heavy metal ion in adsorptive membrane filtration using a metal-organic framework incorporated nanofibrous membrane. *Chem. Eng. J.* **2018**, *352*, 737−744.

(10) Efome, J. E.; Rana, D.; Matsuura, T.; Lan, C. Q. Effects of operating parameters and coexisting ions on the efficiency of heavy metal ions removal by nano-fibrous metal-organic framework membrane filtration process. *Sci. Total Environ.* **2019**, *674*, 355−362.

(11) Efome, J. E.; Rana, D.; Matsuura, T.; Lan, C. Q. Metal-organic frameworks supported on nanofibers to remove heavy metals. *J. Mater. Chem. A* **2018**, *6*, 4550−4555.

(12) Ifuku, S. Chitin and Chitosan Nanofibers: Preparation and chemical modifications. *Molecules* **2014**, *19*, 18367−18380.

(13) Kim, H.-J.; Park, S. J.; Park, C. S.; Le, T.-H.; Hun Lee, S.; Ha, T. H.; Kim, H.-i.; Kim, J.; Lee, C.-S.; Yoon, H.; Kwon, O. S. Surface-modified polymer nanofiber membrane for high-efficiency microdust capturing. *Chem. Eng. J.* **2018**, *339*, 204−213.

(14) Ju, X.; Lu, J.-P.; Zhao, L.-L.; Lu, T.-D.; Cao, X.-L.; Jia, T.-Z.; Wang, Y.-C.; Sun, S.-P. Electrospun transition layer that enhances the structure and performance of thin-film nanofibrous composite membranes. *J. Membr. Sci.* **2021**, *620*, 118927.

(15) Lu, T.-D.; Zhao, L.-L.; Yong, W. F.; Wang, Q.; Duan, L.; Sun, S.-P. Highly solvent-durable thin-film molecular sieve membranes with insoluble polyimide nanofibrous substrate. *Chem. Eng. J.* **2021**, *409*, 128206.

(16) Zhang, Y.; Guo, J.; Han, G.; Bai, Y.; Ge, Q.; Ma, J.; Lau, C. H.; Shao, L. Molecularly soldered covalent organic frameworks for ultrafast precision sieving. *Sci. Adv.* **2021**, *7*, 1−10.

(17) Zhao, Y.; Zhang, Y.; Li, F.; Bai, Y.; Pan, Y.; Ma, J.; Zhang, S.; Shao, L. Ultra-robust superwetting hierarchical membranes constructed by coordination complex networks for oily water treatment. *J. Membr. Sci.* **2021**, *627*, 119234.

(18) Zhang, Y.; Cheng, X.; Jiang, X.; Urban, J. J.; Lau, C. H.; Liu, S.; Shao, L. Robust natural nanocomposites realizing unprecedented ultrafast precise molecular separations. *Mater. Today* **2020**, *36*, 40−47.

(19) Kang, Y. H.; Ahn, K.; Jeong, S. Y.; Bae, J. S.; Jin, J. S.; Kim, H. G.; Hong, S. W.; Cho, C. R. Effect of plasma treatment on surface chemical-bonding states and electrical properties of polyacrylonitrile nanofibers. *Thin Solid Films* **2011**, *519*, 7090−7094.

(20) Savoji, H.; Rana, D.; Matsuura, T.; Tabe, S.; Feng, C. Development of plasma and/or chemically induced graft co-polymerized electrospun poly(vinylidene fluoride) membranes for solute separation. *Sep. Purif. Technol.* **2013**, *108*, 196−204.

(21) Mozaffari, A.; Parvinzadeh Gashti, M.; Mirjalili, M.; Parsania, M. Argon and argon-oxygen plasma surface modification of gelatin nanofibers for tissue engineering applications. *Membranes* **2021**, *11*, 31.

(22) Yalcinkaya, F. Effect of argon plasma treatment on hydrophilic stability of nanofiber webs. *J. Appl. Polym. Sci.* **2018**, *135*, 46751.

(23) Padil, V. V. T.; Stuchlík, M.; Černík, M. Plasma modified nanofibres based on gum kondagogu and their use for collection of nanoparticulate silver, gold and platinum. *Carbohydr. Polym.* **2015**, *121*, 468−476.

(24) Boyraz, E.; Yalcinkaya, F. Hydrophilic surface-modified PAN nanofibrous membranes for efficient oil−water emulsion separation. *Polymers* **2021**, *13*, 197.

(25) Bode-Aluko, C. A.; Pereao, O.; Ndayambaje, G.; Petrik, L. Adsorption of toxic metals on modified polyacrylonitrile nanofibres: a review. *Water, Air, Soil Pollut.* **2017**, *228*, 35.

(26) Hamideh Mortazavi, S.; Pilehvar, S.; Ghoranneviss, M.; Hosseinnejad, M. T.; Zargham, S.; Mirarefi, A. A.; Mirarefi, A. Y. Plasma oxidation and stabilization of electrospun polyacrylonitrile nanofiber for carbon nanofiber formation. *Appl. Phys. A: Mater. Sci. Process.* **2013**, *113*, 703−712.

(27) Iritani, E.; Mukai, Y.; Hagihara, E. Measurements and evaluation of concentration distributions in filter cake formed in dead-end ultrafiltration of protein solutions. *Chem. Eng. Sci.* **2002**, *57*, 53−62.

(28) Iritani, E.; Mukai, Y.; Toyoda, Y. Properties of a filter cake formed in dead-end microfiltration of binary particulate mixtures. *J. Chem. Eng. Jpn.* **2002**, *35*, 226−233.

(29) Iritani, E.; Mukai, Y.; Kamiya, M.; Katagiri, N. Properties of a filter cake formed in dead-end microfiltration of colloidal particles suspended in aqueous organic solvents. *J. Chem. Eng. Jpn.* **2005**, *38*, 271−277.

(30) Furuta, M.; Mukai, Y.; Iritani, E. Control of structure of thin filter cake formed by PSL particles. *Filtration* **2006**, *6*, 163−168.

(31) Bolton, G. R.; LaCasse, D.; Lazzara, M. J.; Kuriyel, R. The fiber-coating model of biopharmaceutical depth filtration. *AIChE J.* **2005**, *51*, 2978−2987.

(32) Cheng, Y.-L.; Lee, D.-J.; Lai, J.-Y. Filtration blocking laws: revisited. *J. Taiwan Inst. Chem. Eng.* **2011**, *42*, 506−508.

(33) Iritani, E. A review on modeling of pore-blocking behaviors of membranes during pressurized membrane filtration. *Drying Technol.* **2013**, *31*, 146−162.

(34) Ho, C.-C.; Zydney, A. L. A combined pore blockage and cake filtration model for protein fouling during microfiltration. *J. Colloid Interface Sci.* **2000**, *232*, 389−399.

(35) Iritani, E.; Mukai, Y.; Furuta, M.; Kawakami, T.; Katagiri, N. Blocking resistance of membrane during cake filtration of dilute suspensions. *AIChE J.* **2005**, *51*, 2609−2614.

(36) Bolton, G.; LaCasse, D.; Kuriyel, R. Combined models of membrane fouling: development and application to microfiltration and ultrafiltration of biological fluids. *J. Membr. Sci.* **2006**, *277*, 75−84.

(37) Ruth, B. F. Studies in Filtration. III. Derivation of general filtration Equations. *Ind. Eng. Chem.* **1935**, *27*, 708−723.

(38) Hermans, P. H.; Bredée, H. L. Principles of the mathematical treatment of constant-pressure filtration. *J. Soc. Chem. Ind.* **1936**, *55*, 1−4.

(39) Iritani, E.; Watanabe, T.; Murase, T. Effects of pH and solvent density on dead-end upward ultrafiltration. *J. Membr. Sci.* **1992**, *69*, 87−97.

(40) Ismail, M. F.; Islam, M. A.; Khorshidi, B.; Sadrzadeh, M. Prediction of surface charge properties on the basis of contact angle titration models. *Mater. Chem. Phys.* **2021**, *258*, 123933.

(41) Kelly, B. S.; Splittgerber, A. G. The Pythagorean theorem and the solid state. *J. Chem. Educ.* **2005**, *82*, 756−761.

(42) Ko, W. L. Deformations of foamed elastomers. *J. Cell. Plast.* **1965**, *1*, 45−50.

(43) Chen, H.; Huang, M.; Liu, Y.; Meng, L.; Ma, M. Functionalized electrospun nanofiber membranes for water treatment: a review. *Sci. Total Environ.* **2020**, *739*, 139944.

(44) Bae, J.; Baek, I.; Choi, H. Mechanically enhanced PES electrospun nanofiber membranes (ENMs) for microfiltration: the effects of ENM properties on membrane performance. *Water Res.* **2016**, *105*, 406−412.

(45) Terpilowski, K.; Rymuszka, D. Surface properties of glass plates activated by air, oxygen, nitrogen and argon plasma. *Glass Phys. Chem.* **2016**, *42*, 535−541.

(46) Correia, D. M.; Ribeiro, C.; Botelho, G.; Borges, J.; Lopes, C.; Vaz, F.; Carabineiro, S. A. C.; MacHado, A. V.; Lanceros-Méndez, S. Superhydrophilic poly(L-lactic acid) electrospun membranes for biomedical applications obtained by argon and oxygen plasma treatment. *Appl. Surf. Sci.* **2016**, *371*, 74−82.

(47) Wang, J.; Chen, X.; Reis, R.; Chen, Z.; Milne, N.; Winther-Jensen, B.; Kong, L.; Dumée, L. Plasma modification and synthesis of membrane materials—a mechanistic review. *Membranes* **2018**, *8*, 56.

(48) Wang, C. X.; Ren, Y.; Qiu, Y. P. Penetration depth of atmospheric pressure plasma surface modification into multiple layers of polyester fabrics. *Surf. Coat. Technol.* **2007**, *202*, 77−83.

(49) Michlíček, M.; Manakhov, A.; Dvořáková, E.; Zajíčková, L. Homogeneity and penetration depth of atmospheric pressure plasma polymerization onto electrospun nanofibrous mats. *Appl. Surf. Sci.* **2019**, *471*, 835−841.

(50) Wang, C. X.; Liu, Y.; Xu, H. L.; Ren, Y.; Qiu, Y. P. Influence of atmospheric pressure plasma treatment time on penetration depth of surface modification into fabric. *Appl. Surf. Sci.* **2008**, *254*, 2499−2505.

(51) Hegemann, D.; Hanselmann, B.; Guimond, S.; Fortunato, G.; Giraud, M.-N.; Guex, A. G. Considering the degradation effects of amino-functional plasma polymer coatings for biomedical application. *Surf. Coat. Technol.* **2014**, *255*, 90−95.

(52) Tucker, B. S.; Baker, P. A.; Xu, K. G.; Vohra, Y. K.; Thomas, V. Atmospheric pressure plasma jet: a facile method to modify the intimal surface of polymeric tubular conduits. *J. Vac. Sci. Technol., A* **2018**, *36*, 04F404.

(53) Bacharouche, J.; Haidara, H.; Kunemann, P.; Vallat, M.-F.; Roucoules, V. Singularities in hydrophobic recovery of plasma treated polydimethylsiloxane surfaces under non-contaminant atmosphere. *Sens. Actuators, A* **2013**, *197*, 25−29.

(54) Wavhal, D. S.; Fisher, E. R. Hydrophilic modification of polyethersulfone membranes by low temperature plasma-induced graft polymerization. *J. Membr. Sci.* **2002**, *209*, 255−269.

(55) Crintea, D. L.; Czarnetzki, U.; Iordanova, S.; Koleva, I.; Luggenhölscher, D. Plasma diagnostics by optical emission spectroscopy on argon and comparison with Thomson scattering. *J. Phys. D: Appl. Phys.* **2009**, *42*, 045208.

(56) Qayyum, A.; Zeb, S.; Ali, S.; Waheed, A.; Zakaullah, M. Optical emission spectroscopy of abnormal glow region in nitrogen plasma. *Plasma Chem. Plasma Process.* **2005**, *25*, 551−564.

(57) Sun, M.; Cai, L. J. Diagnosis of OH radicals in air negative pulsed discharge with nozzle-cylinder electrode by optical emission spectroscopy. *IEEE Trans. Plasma Sci.* **2012**, *40*, 1395−1398.

(58) Saxena, N.; Prabhavathy, C.; De, S.; DasGupta, S. Flux enhancement by argon-oxygen plasma treatment of polyethersulfone membranes. *Sep. Purif. Technol.* **2009**, *70*, 160−165.

(59) Yalcinkaya, F.; Yalcinkaya, B.; Pazourek, A.; Mullerova, J.; Stuchlik, M.; Maryska, J. Surface modification of electrospun PVDF/

PAN nanofibrous layers by low vacuum plasma treatment. *Int. J. Polym. Sci.* **2016**, *2016*, 1.

(60) Wu, M.; Wang, Q.; Li, K.; Wu, Y.; Liu, H. Optimization of stabilization conditions for electrospun polyacrylonitrile nanofibers. *Polym. Degrad. Stab.* **2012**, *97*, 1511−1519.

(61) Wang, Y.; Górecki, R. P.; Stamate, E.; Norrman, K.; Aili, D.; Zuo, M.; Guo, W.; Hélix-Nielsen, C.; Zhang, W. Preparation of super-hydrophilic polyphenylsulfone nanofiber membranes for water treatment. *RSC Adv.* **2019**, *9*, 278−286.

(62) Jordá-Vilaplana, A.; Fombuena, V.; García-García, D.; Samper, M. D.; Sánchez-Nácher, L. Surface modification of polylactic acid (PLA) by air atmospheric plasma treatment. *Eur. Polym. J.* **2014**, *58*, 23−33.

(63) Kedroňová, E.; Zajíčková, L.; Hegemann, D.; Klíma, M.; Michlíček, M.; Manakhov, A. Plasma enhanced CVD of organosilicon thin films on electrospun polymer nanofibers. *Plasma Processes Polym.* **2015**, *12*, 1231−1243.

(64) Das, P.; Ojah, N.; Kandimalla, R.; Mohan, K.; Gogoi, D.; Dolui, S. K.; Choudhury, A. J. Surface modification of electrospun PVA/chitosan nanofibers by dielectric barrier discharge plasma at atmospheric pressure and studies of their mechanical properties and biocompatibility. *Int. J. Biol. Macromol.* **2018**, *114*, 1026−1032.